Rectilinear six-dimensional ionization cooling channel for a muon collider: A theoretical and numerical study

Diktys Stratakis and Robert B. Palmer

Brookhaven National Laboratory, Upton, New York 11973, USA

(Received 25 September 2014; published 6 March 2015)

A muon collider requires a reduction of the six-dimensional emittance of the captured muon beam by several orders of magnitude. In this study, we describe a novel rectilinear cooling scheme that should meet this requirement. First, we present the conceptual design of our proposed scheme wherein we detail its basic features. Then, we establish the theoretical framework to predict and evaluate the performance of ionization cooling channels and discuss its application to our specific case. Finally, we present the first end-to-end simulation of 6D cooling for a muon collider and show a notable reduction of the 6D emittance by 5 orders of magnitude. We find good agreement between simulation and theory.

DOI: 10.1103/PhysRevSTAB.18.031003 PACS numbers: 29.20.Ej, 41.75.Lx

I. INTRODUCTION

Lepton (e^+e^-) colliders have the valuable property of producing simple, single-particle interactions with little background, and this property is essential in the exploration of new particle states. However, extension of (e^+e^-) colliders to multi-TeV energies is performance constrained by radiative effects and cost constrained because two full energy linacs are required [1]. Since radiative energy losses for a lepton of mass m are inversely proportional to m^4 [2], radiation difficulties may be circumvented by use of a heavier probe. For this reason, it seems prudent to more concretely investigate muon beams as primary probes in high-energy collisions, since they combine an electronlike nature with a large mass which is sufficiently immune to radiation [3–5].

The initial muon beam occupies a relatively large phase-space volume which must be compressed by several orders of magnitude to obtain high-luminosity collisions [6]. Furthermore, this phase-space reduction must be done within a time that is not long compared to the muon lifetime (2 μs in rest frame). Ionization cooling is currently the only feasible option for cooling a muon beam [7,8]. This technique is not very practical for protons, which would have frequent nuclear interactions, or electrons, which would have bremsstrahlung, but is practical for muons, and cooling rates compatible with muon lifetimes are possible.

Ionization cooling is achieved by reducing the beam momentum through ionization energy loss in absorbers and replenishing the momentum loss only in the longitudinal direction through rf cavities. This mechanism can effectively reduce the transverse phase space of a beam in the same way as radiation damping does to an electron beam. However it does not effectively cool the longitudinal momentum spread because the energy-loss rate is not sensitive to beam momentum except for very low-energy muons. In order to reduce the longitudinal emittance, the so-called "emittance exchange" [9] technique is commonly used, where a dispersive beam is passed through a discrete [10,11] or continuous absorber [12] in such a way that the high-energy particles traverse more material than the low-energy particles. The net result is a reduction of the longitudinal emittance at the cost of simultaneously increasing the transverse emittance. By controlling the amount of emittance exchange the six-dimensional emittance can be reduced.

Ionization cooling of muons seems relatively straightforward in theory, but will require extensive simulation and feasibility studies for its optimization. The main goal of this paper is to develop a potential baseline cooling lattice for a muon collider and evaluate its performance. In order to accomplish this, we follow a sequence of steps. First, we present a novel rectilinear lattice design that in view of its simple geometry may offer several technological advantages for muon cooling over previously considered schemes [13,14]. Second, we review the theoretical framework to evaluate the efficiency of ionization cooling channels and discuss its application to our present rectilinear scheme. We use the basic theory to predict the cooling rate and identify the most promising lattice properties such as the absorber length, rf frequency and focusing arrangement that is within the practical limits on magnetic field strengths. Finally, we numerically examine the performance of the channel with ICOOL [15], a standard code that fully incorporates all basic physical processes such as energy loss, scattering, straggling and muon decay. We initiate our simulation at the front end of a proposed Neutrino factory [16] and present for the first time a detailed end-to-end simulation.

Key parameters, such as the transverse and longitudinal cooling emittances, are compared against findings from theoretical calculations. We find good agreement between simulation and theory and show that with a rectilinear channel a notable 6D emittance decrease by more than 5 orders of magnitude can be achieved.

The outline of this paper is as follows: In Sec. II, we give a brief overview of some previously considered ionization cooling schemes. In Sec. III, we provide details of the design parameters for the proposed rectilinear channel. Next, in Sec. IV we review the fundamental ionization cooling theory. In Sec. V we report the results from our simulations modeling the aforementioned channel and compare them with the theoretical values. Finally, we present our conclusions in Sec. VI. We note that the subject of this study will be lattices with discrete absorbers, only.

II. SOME ALTERNATIVE 6D COOLING SCHEMES

Three different geometries for ionization cooling towards micron-scale emittances as required for a muon collider have been previously considered. The common feature for all cases was that the solenoids were slightly tilted to generate upward dipole fields. In the first, shown in Fig. 1(a), the lattice is bent into a circle, with the curvature corresponding to that generated by the dipole components [17,18]. The ring consists of a series of identical cells with two or four solenoids in each cell with opposite polarity to provide transverse focusing. The coils (yellow) are not evenly spaced; those on either side of the wedge absorber (magenta) are closer together in order to increase the focusing at the absorber and thus minimizing the beta function at that location. The relative amount of cooling can be adjusted by changing the opening angle and transverse location of the wedge. A series of rf cavities (dark red) are used to restore the momentum along the longitudinal axis. The dispersion necessary for emittance exchange is provided from the bend field generated by tilting the axes of the solenoids above and below the orbital midplane. Simulations have shown that a suitable sequence of such rings, with multiple stages using different cell lengths, focusing fields, and rf frequencies, can provide 2 orders of magnitude reduction of the normalized phase-space volume with a transmission above 50%. However, injection into or extraction from such rings would be very challenging.

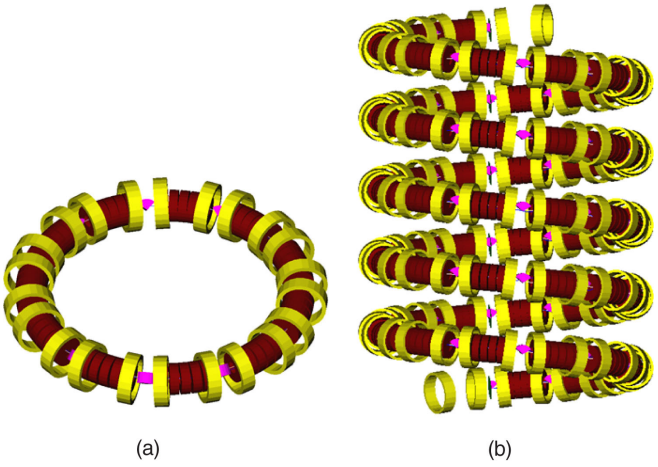

FIG. 1. Some previously considered 6D ionization cooling lattices: (a) Schematic layout of a ring cooler; (b) 5 turn slice of a Guggenheim helix. The large yellow cylinders are solenoids, the small red cylinders are the active volume of the rf cavities, and the magenta wedges are hydrogen absorbers.

In the second case, represented in Fig. 1(b), the cooling cells are set on a gently upward or downward helix (as in the New York Guggenheim Museum and commonly referred to by that name). Simulations [19] have shown that their performance is almost the same as that of rings of the same approximate bending radii. This case would appear to be practical for the early stages of 6D cooling, but would be increasingly difficult as the radii get smaller in the later stages. An added complication is that stray fields from one pitch can influence those before and after, causing the beam to be heavily distorted.

In the third case, essentially the same cells from a ring or a Guggenheim, including their coil tilts and resulting upward dipole fields, are laid out in straight (rectilinear) geometry. The solenoid focusing is so strong, compared with the dipole deflections, that the closed orbits are merely displaced laterally, but continue down the now straight lattice. This rectilinear scheme was proposed for the first time by Balbekov [20] and is represented in Fig. 2. Despite its much simpler geometry, it was found [21] that its cooling performance was essentially the same as with rings

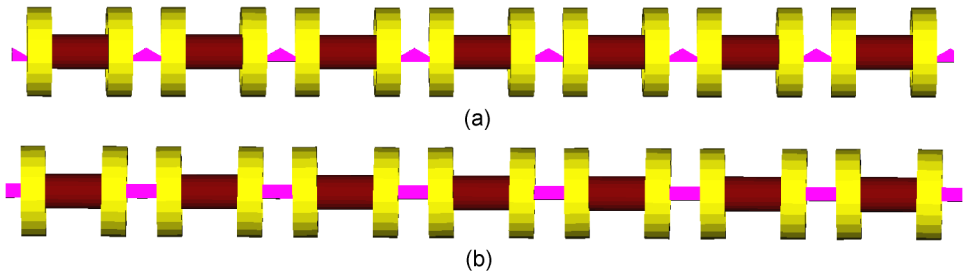

FIG. 2. Conceptual design of a rectilinear channel: (a) top view; (b) side view.

or a helix. As a result, the rectilinear scheme will be considered our new baseline cooling lattice and will be analyzed in more detail in the next section.

III. RECTILINEAR CHANNEL: LATTICE DESIGN

A complete scheme for cooling a muon beam sufficiently for use in a muon collider has been previously described [6]. The proposed scheme consists of a sequence of steps. The first step, referred to as phase rotation [16] converts the initial single muon bunch with very large energy spread into a train of bunches with much reduced spread of which we use only 21. The next step uses an ionization cooling channel to reduce the 6D emittance of the bunch train until it can be injected into a bunch-merging system. The single muon bunches, one of each sign, are then sent through a second 6D cooling channel where the transverse emittance is reduced as much as possible and the longitudinal emittance is cooled to a value below that needed for the collider. If necessary, the beam can be sent through a final 4D cooling channel using high-field solenoids that further cools the transverse emittance while allowing the longitudinal emittance to grow. While well-defined concepts on the phase-rotation [16], charge separation [22,23] and bunch merger [24–26] subsystems have been previously reported, the conceptual design and simulation of a 6D cooling channel suitable for a muon collider is far from complete. Therefore, the focus of this paper will be the 6D system, before and after the bunch recombination. Unlike most previous studies where *a priori* assumption of the initial beam distribution was made [27] and/or a modest cooling was achieved [14,28], in this study we present a detailed end-to-end simulation by using the actual post-phase-rotation beam and show that our channel has the potential to cool towards the baseline emittance requirement for a muon collider.

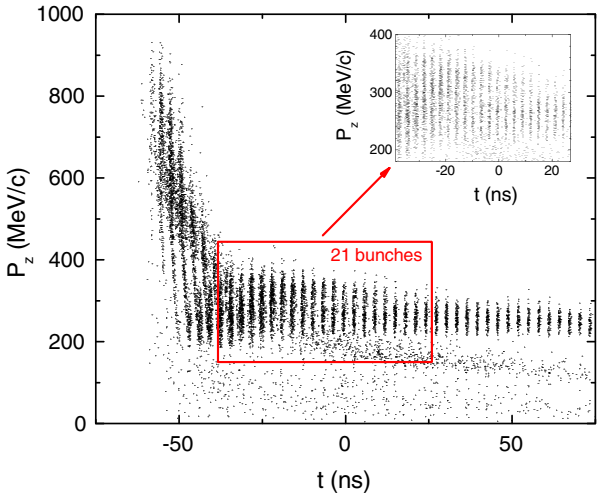

FIG. 3. Longitudinal phase space of a muon beam after phase rotation and just before entering the cooling channel. The phase rotation converts the initial single muon bunch with large energy spread into a train of bunches with much reduced energy spread of which we use only 21. The muons enclosed within the red box are also shown in Fig. 8(a).

A. Cooling before bunch recombination

The scheme starts with the post-phase-rotation beam that yields bunch trains of muons and is illustrated in Fig. 3. Recent studies [29] showed that good cooling efficiency requires the channel to be tapered. As a result, parameters such as the cell length, focusing strength and rf frequency change from stage to stage based on the emittance reduction rate and transmission with the purpose to maintain a beam emittance that is always larger from the equilibrium emittance.

We consider a four-stage (A1–A4) tapered channel, where each stage consists of a sequence of identical cells and some of the main lattice parameters are summarized in Table I. At the first stage of the channel, the focusing will be relatively weak to avoid excessive angular divergence that can arise from the large transverse emittance of the initial beam. This stage is then terminated and we couple into the next stage that has a lower beta. This is achieved by simultaneously scaling down the cell dimensions and raising the strength of the on-axis solenoidal field. A common feature of all stages is that they consist of equally spaced alternating solenoids (commonly known as FOFO lattices) so that they can operate above the π resonance and thus have the highest possible momentum acceptance.

Figure 4(a) shows the side view of one cell of the first stage of the channel (stage A1). This stage consists of a sequence of 66 identical 200 cm cells, each containing six 25.5 cm-long 325 MHz pillbox cavities, and two wedge-shaped liquid hydrogen (LH) absorbers, with 12.2 cm central thickness and 39 degree opening angle. Moreover, each cell contains two solenoid coils of opposite polarity, yielding an approximate sinusoidal variation of the magnetic field in the channel with a peak on-axis value of 2.4 T. The minimum value of the transverse beta function β_T, is 72.7 cm (at 200 MeV/c) and occurs at the absorber center. The solenoids are tilted in opposite directions by 3.1 degrees providing a 10.7 cm dispersion at the absorber center which is mainly along the x axis. The peak accelerating gradient of the rf cavities is 22 MV/m, while each operates at a synchronous phase 14 degrees off the 0-crossing point.

Figure 4(b) shows the last cooling stage (stage A4) that is designed for late stage cooling towards the bunch-merging system [24–26] which requires a normalized transverse rms emittance $\leq$1.5 mm and a normalized longitudinal rms emittance $\leq$2.5 mm. In order to reach this goal, the transverse beta function at the absorbers has to be reduced from $\sim$72 to $\sim$27 cm. This reduction, without changing the essential dynamics, is achieved by scaling down the cell length (from 200 to 80 cm) and proportionally raising the peak axial field (from 2.4 to 6.0 T). Stage A4 consists of 88

TABLE I. Main parameters of a 12-stage rectilinear 6D cooling lattice before and after recombination. Stages A1–A4 and B1–B4 use LH absorber while stages B5–B8 use LiH absorber. Dispersion is calculated at the absorber center at the reference momentum of 200 MeV/c.

Stage	Cell length [m]	Total length [m]	rf frequency [MHz]	rf gradient [MV/m]	rf #	rf length [cm]	Coil tilt [deg]	Pipe radius [cm]	Dispersion [cm]	Wedge angle [deg]
A1	2.000	132.00	325	22.0	6	25.50	3.1	30.0	10.7	39
A2	1.320	171.60	325	22.0	4	25.00	1.8	25.0	6.8	44
A3	1.000	107.00	650	28.0	5	13.49	1.6	19.0	4.2	100
A4	0.800	70.40	650	28.0	4	13.49	0.7	13.2	1.9	110
B1	2.750	55.00	325	19.0	6	25.00	0.9	28.0	5.2	120
B2	2.000	64.00	325	19.5	5	24.00	1.3	24.0	5.0	117
B3	1.500	81.00	325	21.0	4	24.00	1.1	18.0	4.6	113
B4	1.270	63.50	325	22.5	3	24.00	1.1	14.0	4.0	124
B5	0.806	73.35	650	27.0	4	12.00	0.7	9.0	1.4	61
B6	0.806	62.06	650	28.5	4	12.00	0.7	7.2	1.2	90
B7	0.806	40.30	650	26.0	4	12.00	0.8	4.9	1.1	90
B8	0.806	49.16	650	28.0	4	10.50	0.6	4.5	0.6	120

cells, each containing four 650 MHz cavities and one LH wedge absorber to produce the energy loss as before. The increase in frequency allows a raise in the operating gradient from 22 to 28 MV/m. This change reduces the relative fraction of length needed for the rf and gives more space for solenoidal coils. By carefully examining Figs. 4(a) and 4(b) and Table I the following points are noteworthy: First, the dispersion at the cell entrance of

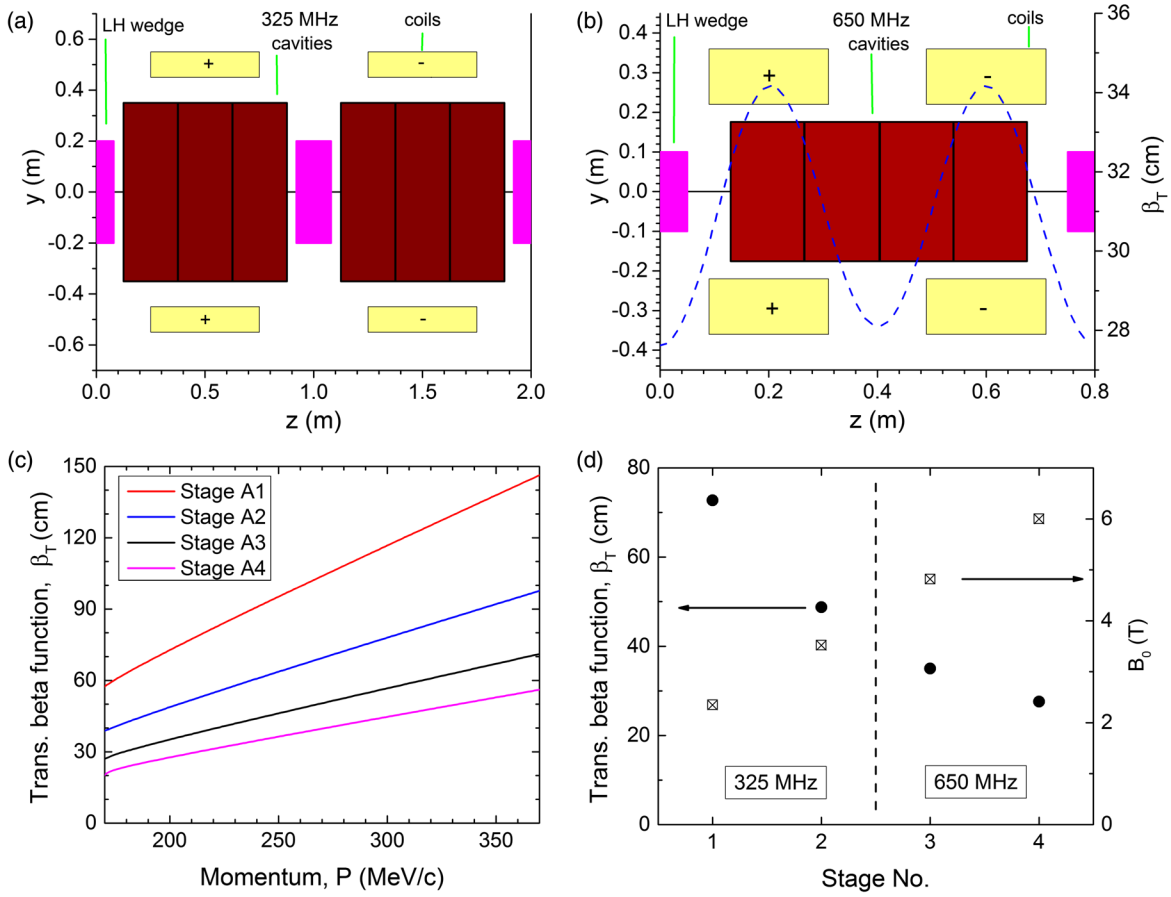

FIG. 4. Lattice characteristics of the rectilinear 6D cooling channel before bunch recombination: (a) side view of one cell of the first stage (stage A1); (b) side view of one cell of the last stage (stage A4). The dashed curve shows the beta function versus z in the cell at 200 MeV/c; (c) beta function versus momentum; (d) beta function at the absorber center (dark circles) at 200 MeV/c and peak-on-axis magnetic field (squares) for all stages. The tilts of solenoids are not shown.

stage A4 is almost 5 times smaller than in stage A1, which is a direct consequence of the stronger focusing field. As we will show in more detail in Sec. V, this value is adequate enough to provide the required longitudinal cooling. Second, a common feature for all stages is that the absorbers are located at beta minima. For stage A4, this is illustrated by the blue dashed curve in Fig. 4(b) which shows the dependence of the beta function with position. Since the lattice equilibrium emittance is proportional to the beta function [8], placing the absorber on that location would enhance the cooling rate compared to any other location in the cell.

Figure 4(c) shows the transverse beta function versus momentum for all stages. As also noted earlier, all stages are carefully designed so that they can operate above the π resonance and thus have the highest possible momentum acceptance. This is necessary since a glance at Fig. 3 indicates that the post-phase-rotator beam has a wide momentum spread. Finally, Fig. 4(d) exhibits the transverse beta function at the absorber center and peak-on-axis magnetic field for all stages. As desired, the field is becoming progressively stronger so as to enhance the cooling rate by reducing the beta function and hence the equilibrium emittance.

B. Cooling after bunch recombination

Previous studies [24–26] showed that after bunch merging, both longitudinal and transverse emittances of the now single muon bunch increase by a factor ~4 and thus are comparable to their initial values. It can thus be taken again through the same cooling system but with one important difference. While only a modest transverse cooling to ~1.5 mm was required before the bunch-merging system, the new single muon bunch needs to be cooled by an additional order of magnitude before it can be sent to the accelerator systems. This implies that the beta function at the late stages needs to be very small (≤5.0 cm). Given the

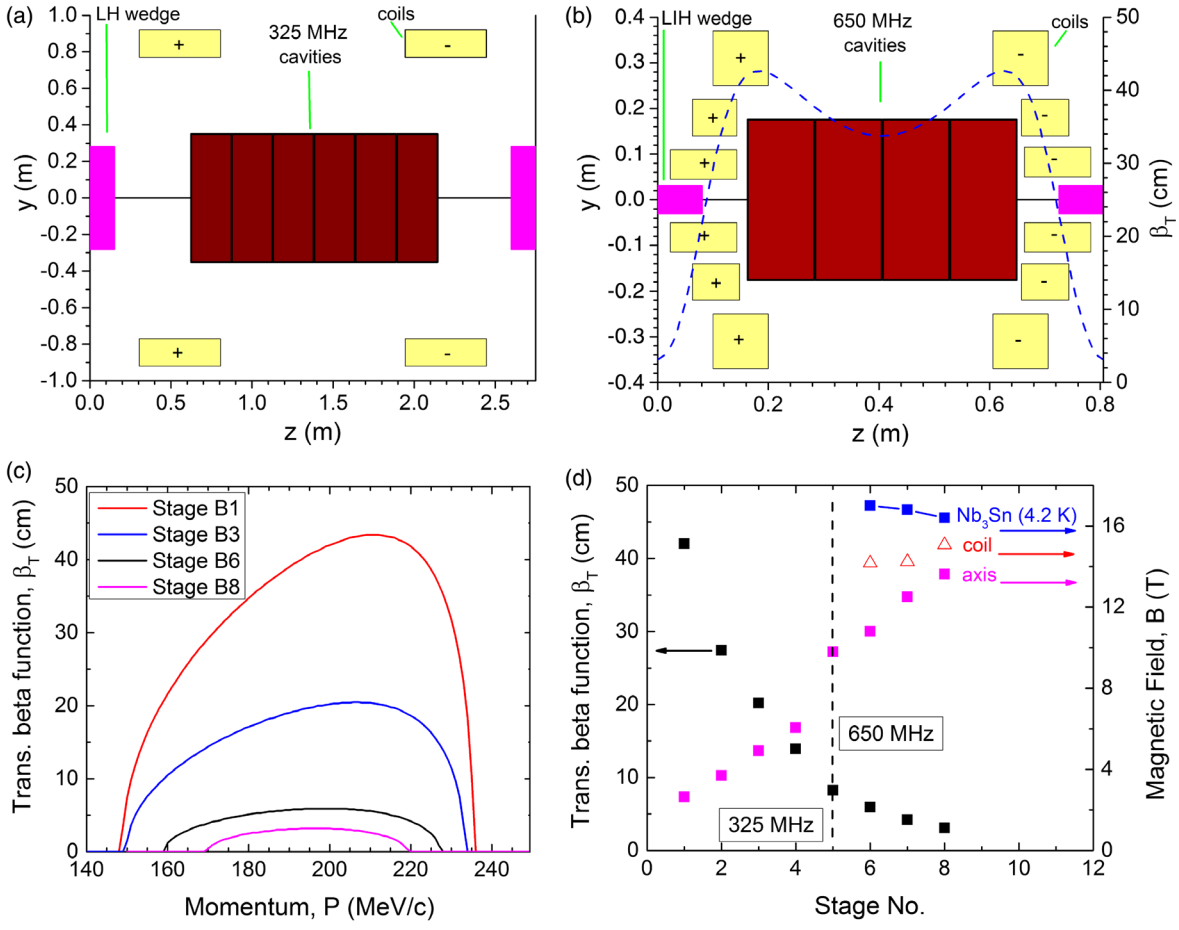

FIG. 5. Lattice characteristics of the rectilinear 6D cooling channel after bunch recombination: (a) side view of one cell of the first stage (stage B1); (b) side view of one cell of the last stage (stage B8). The dashed curve shows the beta function versus z in the cell at 200 MeV/c; (c) beta function versus momentum; (d) beta function at the absorber center (at 200 MeV/c) and peak-on-axis magnetic field for all stages. The triangles depict the maximum field in the coil, while the squares show the maximum allowable field at the used coil current density, assuming an Nb_3Sn conductor. The used current densities are 185 A/mm^2 (stage B6), 198 A/mm^2 (stage B7) and 220 A/mm^2 (stage B8). The tilts of solenoids are not shown.

practical limits on magnetic field strengths, this makes the whole scheme quite challenging.

We consider eight tapered stages (B1–B8) to achieve this goal and the required lattice parameters are summarized in more detail in Table I. Since good cooling requires that the absorber length along the beam path be comparable with the minimum value of the beta function [27], this becomes impractical with LH and we switched to using lithium hydride (LiH) as the absorber material for stages B5–B8. The aperture was gradually decreasing along the channel (see Table I) in order to accommodate the higher frequency rf cavities for the later stages. Figure 5(a) shows a cross section of a cell of the first stage (stage B1). The rf is at 325 MHz operating at 19 MV/m and a phase of approximately 41 degrees. The cell contains two coils of opposite polarity, yielding an approximate sinusoidal variation of the magnetic field in the channel with a peak on-axis value of 2.6 T. The coils are tilted in opposite directions by 0.9 degrees. Figure 5(b) shows a cell of the last cooling stage (stage B8) that is required to cool the beam transversely to ≤0.3 mm. The cell consists of six solenoids which surround four 650 MHz cavities in the cell center. As before, the geometry of the lattice is such that the absorber is located at beta minima (blue dashed curve).

Figure 5(c) shows the transverse beta function at the absorber versus momentum for four stages out of the total eight stages of the channel. Since the average momentum of the incoming beam is expected to be within 200–210 MeV/c [26], all stages are appropriately designed so as to provide a central momentum near 200 MeV/c. Notice that the region over which the momentum is nonzero becomes progressively smaller implying a reduction in momentum acceptance as the beam propagates towards the late stages. For instance, while the momentum acceptance is above 80 MeV/c at the first stages, it drops below 60 MeV/c for the last two. From a beam dynamics point of view this is not a point of concern since each stage is carefully designed so as to provide a momentum acceptance that is at least 5 times greater than the sigma of the longitudinal momentum spread.

In a similar fashion with the channel before recombination, the transverse beta function becomes progressively smaller from stage to stage by scaling down the cell dimensions and raising the on-axis magnetic field [Fig. 5(d)]. As a result, the minimum beta function drops from 42.0 to 3.0 cm while the on-axis peak magnetic field increases from 2.6 to 13.6 T. This implies that there is a relatively rapid increase of the magnet operating current with stage number. This can become a challenge since the operating current in a superconducting magnet must be smaller than the critical current corresponding to the peak field in the coil. To highlight this last fact we also plot in Fig. 5(d) the maximum local fields in the coils for the last three stages (triangles) and compare them to the published [31] maximum allowable field (squares) for the used coil current density, assuming a Nb_3Sn conductor. Our findings indicate that the needed fields are consistent with the critical limits of existing conductor technology but the last stages are barely within the limits of Nb_3Sn. Most challenging is stage B8 where the solenoids are expected to deliver 15 T in a bore of 4.5 cm. A recent magnet feasibility study [32,33] revealed that for a more stable operation a 1.9 K operating magnet temperature is preferred for this stage. This would allow the Nb_3Sn inner solenoids to operate at 85% of the load line at operational current.

IV. RECTILINEAR CHANNEL: BASIC THEORY

In ionization cooling, particles pass through a material medium and lose energy through ionization interactions, and this is followed by beam reacceleration in rf cavities. The losses are parallel to the particle motion, and therefore include transverse and longitudinal momentum losses; the reacceleration restores only longitudinal momentum. The net loss of momentum reduces the transverse beam emittance and thus is cooling the beam. However, the random process of multiple scattering in the material medium increases the rms beam divergence, adding a heating term which must be controlled in a complete cooling system.

The differential equation for rms transverse cooling of muons is [4,8,9]

$$\frac{d\varepsilon_T}{ds} = -\frac{g_T}{\beta^2 E}\frac{dE}{ds}\varepsilon_T + \frac{\beta_T E_s^2}{2\beta^3 m_\mu c^2 L_R E}, \tag{1}$$

where the first term is the energy loss cooling effect and the second is the multiple scattering heating term. Here ε_T is the normalized rms emittance, E is the beam energy, β is the particle velocity, c is the speed of light, dE/ds is the energy loss rate, β_T is the transverse betatron function, L_R is the material radiation length and E_S is characteristic scattering energy (~13.6 MeV). The factor $g_T = 1 - D/w$ is the transverse partition number [9,30,34] analogous to the

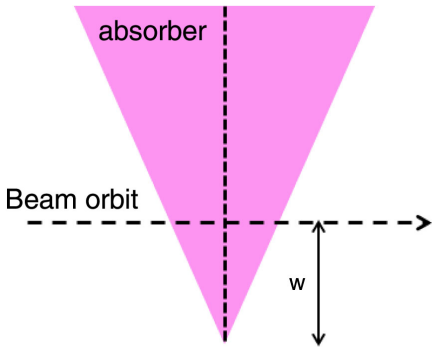

FIG. 6. edge geometry for emittance exchange. With wedges and dispersion, the partition numbers g_T, g_L can be modified but their sum remains constant [30]. For dispersion D and wedge absorbers with height w from the beam to the wedge apex, the transverse partition function becomes $g_T = 1 - D/w$.

partition numbers in synchrotron radiation dumping, D is the dispersion at the absorber and, w is the height from the beam position to the wedge apex (see Fig. 6). Note that in the case of a disk absorber, there is no dispersion and $g_T = 1$.

Neuffer [9,30,35] has given the differential equation for longitudinal cooling in units of energy and phase as follows:

$$\frac{d\varepsilon_L}{ds} = -\frac{g_L}{\beta^2 E}\frac{dE}{ds}\varepsilon_L + \frac{\beta_L}{2}\frac{d\langle\Delta E^2\rangle}{ds}, \tag{2}$$

in which the second term is due energy straggling and β_L is the longitudinal amplitude function in a dimension of reciprocal energy and is defined as [35]

$$\beta_L = \sqrt{\frac{2\pi\alpha_p}{\beta^3\gamma e V' \sin\varphi_s \lambda_{\mathrm{RF}} m_\mu c^2}}, \tag{3}$$

where λ_{RF} is the rf wavelength, V' is the average acceleration gradient, φ_s is the rf phase, and α_p is the momentum compaction which can be approximated by $1/\gamma^2$ where γ is the Lorentz factor. The energy loss can be estimated by the Bethe-Bloch equation [36]:

$$\frac{dE}{ds} = 4\pi N_A r_e^2 m_e c^2 \rho \frac{Z}{A}\left[\frac{1}{\beta^2}\ln(K\gamma^2\beta^2) - 1 - \frac{\delta}{2\beta^2}\right]. \tag{4}$$

Here r_e is the classical electron radius, N_A is the Avogadro's number, ρ is the density, A is the atomic weight, $K = 2m_e c^2/I$, and m_e is the electron mass. The ionization potential is $I \approx 16Z^{0.9}$ eV where Z is the atomic number, and δ is the density effect factor which is small for low-energy muons and assumed to be zero in this study.

In the long path length Gaussian-distribution limit, the second term in Eq. (2) is given approximately by [37]

$$\frac{d\langle\Delta E^2\rangle}{ds} = 4\pi(r_e\gamma m_e c^2)^2 n_e\left(1 - \frac{\beta^2}{2}\right). \tag{5}$$

Here $n_e = \rho N_A Z/A$ is the electron density in the material. This expression increases rapidly with higher energy, opposing the cooling process.

The longitudinal partition number, g_L, consists of two parts, the first is due to the variation of dE/ds with $\beta\gamma$ and the second term is due to the wedge absorbers [35]:

$$g_L = \frac{2\gamma^2 - 2\ln[K(\gamma^2-1)]}{\gamma^2\ln[K(\gamma^2-1)] - (\gamma^2-1)} + \frac{D}{w}. \tag{6}$$

Cooling stops at the equilibrium emittance that we find by putting $d\varepsilon/ds = 0$ in the cooling equations and solving for the emittance. For the transverse emittance we get

$$\varepsilon_T^{\mathrm{eq}} = \left(\frac{dE}{ds}\right)^{-1}\frac{\beta_T E_s^2}{2\beta g_T m_\mu c^2 L_R}. \tag{7}$$

Similarly, an expression for the longitudinal emittance can be obtained:

$$\varepsilon_L^{\mathrm{eq}} = \left(\frac{dE}{ds}\right)^{-1}\frac{\beta^2 E\beta_L}{2g_L}\frac{d\langle\Delta E^2\rangle}{ds}. \tag{8}$$

By averaging the s-dependent quantities in Eqs. (1) and (2), we turn them into first-order differential equations with constant coefficients that we can solve in closed form for both transverse and longitudinal emittances with the appropriate expressions for initial and equilibrium emittances, i.e.,

$$\varepsilon^{\mathrm{calc}}(s) = \varepsilon^{\mathrm{eq}} + (\varepsilon^0 - \varepsilon^{\mathrm{eq}})\exp\left(-\frac{s}{s^{\mathrm{calc}}}\right). \tag{9}$$

Here ε^0 is the initial normalized emittance (transverse or longitudinal) at $s = 0$ and $\varepsilon \to \varepsilon^{\mathrm{eq}}$ for $s \to \infty$ as expected. The quantities s_T^{calc} and s_L^{calc} are the transverse and longitudinal cooling lengths given by the expressions

$$s_T^{\mathrm{calc}} = \frac{\beta^2 E}{g_T}\left\langle\frac{dE}{ds}\right\rangle^{-1}, \tag{10}$$

$$s_L^{\mathrm{calc}} = \frac{\beta^2 E}{g_L}\left\langle\frac{dE}{ds}\right\rangle^{-1}, \tag{11}$$

where the energy loss is averaged over the full transport length. That means dE/ds should be multiplied by the filling factor, i.e., the fraction of the total absorber length over the cooling channel length. Hence, it is enclosed in angular brackets in Eqs. (10) and (11).

V. RECTILINEAR CHANNEL: NUMERICAL STUDY

The performance of the cooling channel was simulated using the ICOOL code [15]. The code includes all relevant physical processes (e.g., energy loss, straggling, multiple scattering) and muon decay. For each stage we generated 3D cylindrical field maps by superimposing the fields from all solenoids in the cell and its neighbor cells. The rf cavities were modeled using cylindrical pillboxes running in the TM010 mode and a reference particle was used to determine each cavity's relative phase. The absorber material was either LH or LiH. The LH absorber was enclosed within 100 μm-thick aluminum safety windows. For simplicity, we assumed that the windows are planar and located axially on both sides of the wedge. Furthermore, their diameter was equal to the pipe aperture.

Figure 7 shows the overall cooling performance as simulated by ICOOL. As noted earlier the new born muon

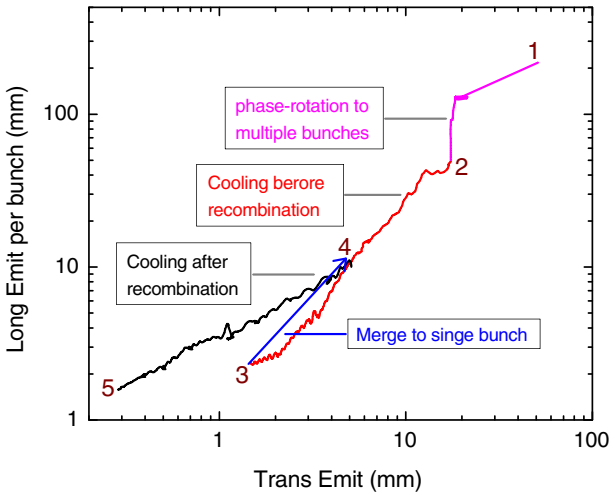

FIG. 7. End-to-end simulation plot of 6D cooling for a muon collider showing the evolution of the longitudinal emittance versus transverse emittance from the capture target to the end of 6D cooling.

beam is first bunched and phase rotated (step #1) so that the initial single bunch with very large energy spread is converted into a train of bunches with much reduced energy spread of which we use 21. Here it is worth mentioning that the muon beam is the result of the impact of 10^6, 8 GeV protons on a liquid mercury target [16]. The post-phase-rotation beam (Fig. 3) contains 272,000 muons and 65% are within the 21 bunches [Figs. 8(a) and 9(a)]. The beam has a normalized transverse emittance of 17.0 mm and a normalized longitudinal emittance of 46.0 mm. The emittances have been obtained using ECALC9 [38], an emittance calculation program customarily employed by the muon accelerator program.

After phase rotation, the beam enters a multistage cooling channel (step #2). We found that the four-stage rectilinear channel described in Sec. III A reduces the transverse emittance by a factor of ~11.5 and the longitudinal emittance by a factor ~19.5. The transmission is 52% including muon decays. More details on the simulated emittance evolution can be found in Table II. Note that at

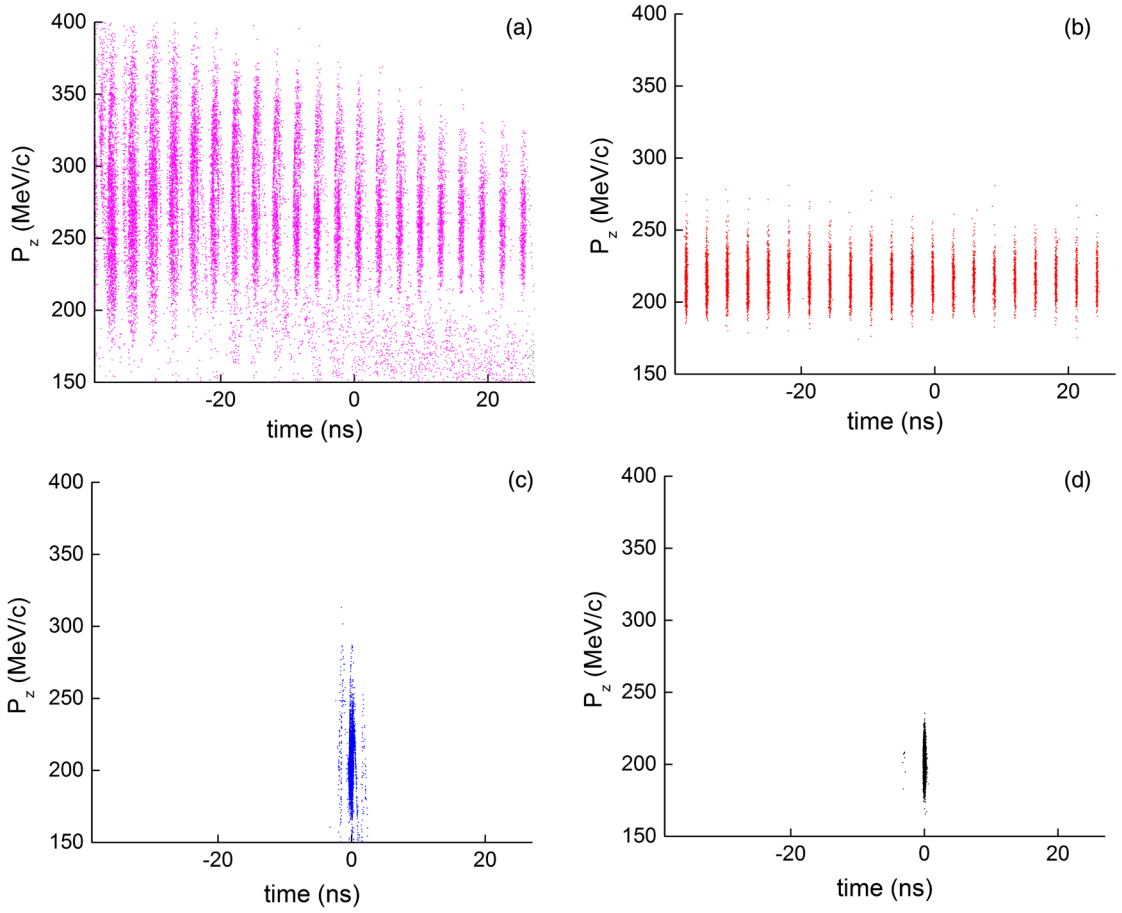

FIG. 8. Snapshots of a sample of the longitudinal phase space at various positions along our proposed 6D rectilinear cooling channel: (a) at the entrance of the cooling channel before recombination; (b) at the entrance of the bunch merger; (c) at the exit of the bunch merger [26]; (d) at the end of the 6D cooling channel.

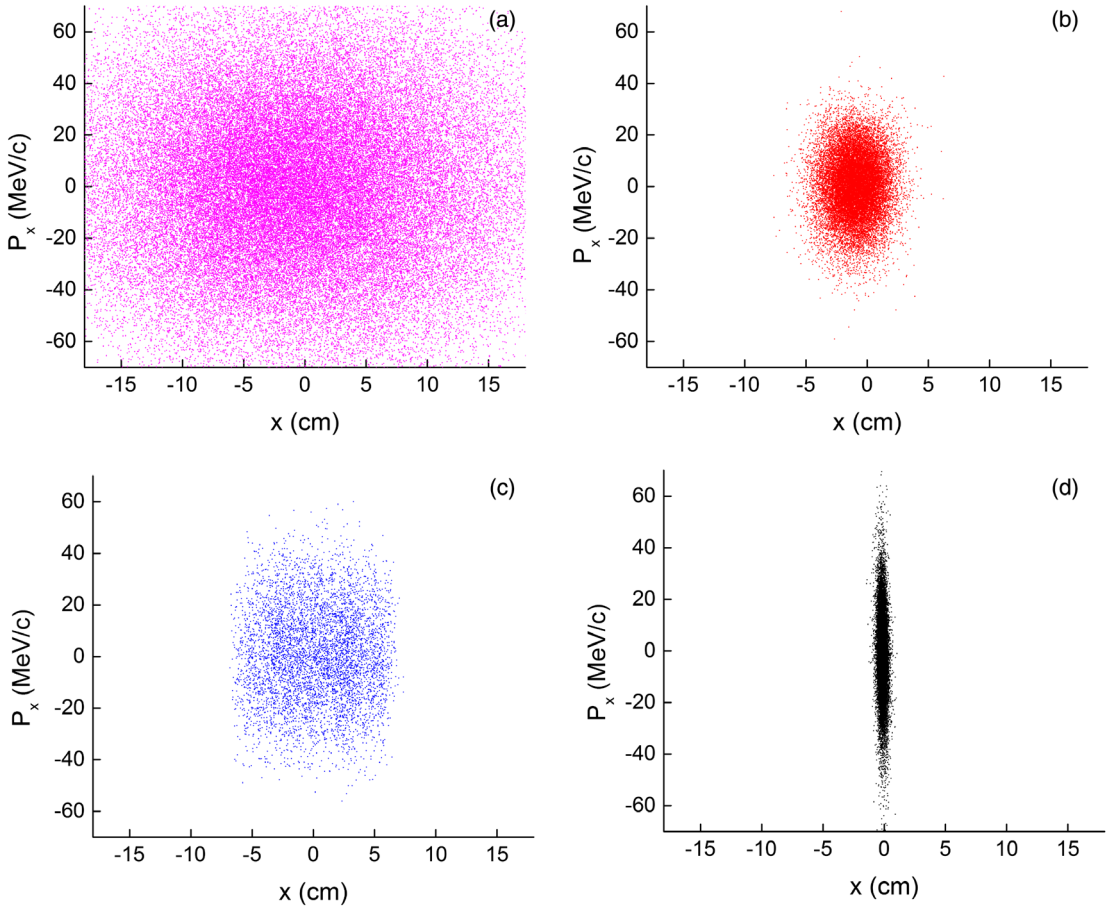

FIG. 9. Snapshots of the transverse phase space at various positions along our proposed 6D rectilinear cooling channel: (a) at the entrance of the cooling channel before recombination; (b) at the entrance of the bunch merger; (c) at the exit of the bunch merger [26]; (d) at the end of the 6D cooling channel.

the end of the premerge channel the transverse emittance is 1.48 mm while the longitudinal emittance is 2.35 mm, which are within the desired values of the bunch merging system [26]. The corresponding longitudinal and transverse phase spaces at that location are shown in Figs. 8(b) and 9(b), respectively. Note from Table II that the average momentum does not remain constant along the channel, but drops progressively from 255 to 215 MeV/c. This will reduce the transverse beta function and thus enhance the cooling performance without the need for excessive focusing.

After the bunch merging (step #3), 15% of the beam is lost while the longitudinal and transverse emittance was found to increase to 10.0 and 5.1 mm, respectively [26]. The now single bunch [Figs. 8(c) and 9(c)] is sent into another multistage channel for further cooling (step #4). We found that the eight-stage rectilinear channel described in Sec. III B reduced the transverse emittance to 0.28 mm and the longitudinal emittance to 1.57 mm [Figs. 8(d) and 9(d)]. At the end of the channel, the transmission was 40% including decays and the average momentum has dropped to 200 MeV/c. Here, it important to recall findings from earlier simulations [39] which revealed severe particle loss and emittance growth due to space charge if the longitudinal emittance drops below 1.50 mm. Thus, to assure satisfactory cooling with minimum losses we choose to cool longitudinally above that limit.

Based on our simulations, 12 cooling stages are sufficient to reduce the transverse and longitudinal emittances by a factor of $\approx 10^2$ and factor of ≈ 10, respectively. As a result the 6D emittance has fallen by a factor of 10^5 with a net transmission of $\sim 20.8\%$ while the overall distance needed to achieve this was ~ 0.96 km. Here, it is worth emphasizing the following important points: First, a normalized transverse emittance ≤ 0.30 mm is the baseline requirement [40] for a muon collider after the final 6D cooling sequence. The results in Fig. 7 suggest that our rectilinear channel has the potential to achieve this goal. Moreover, based on the published parameters of Ref. [41], a muon collider with a luminosity of 1×10^{34} cm^{-2} s^{-1} at 1.5 TeV will require bunches with 2×10^{12} muons on the collider or 4.7×10^{12} muons at the end of 6D cooling for an initial 8 GeV, 4 MW proton driver with 2.1×10^{14} protons per bunch at the target. Using a simple scaling we estimate that the number of muons at the end of 6D cooling for our

TABLE II. Simulation results of the normalized emittance and momentum at the exit of each stage of our proposed rectilinear channel. The last column shows the transmission, T, of each stage.

Stage	$\varepsilon_T^{\mathrm{sim}}$ [mm]	$\varepsilon_L^{\mathrm{sim}}$ [mm]	P_z^{sim} [MeV/c]	T [%]
Begin	17.00	46.00	255	
A1	6.28	14.48	238	70.6
A2	3.40	4.64	229	87.5
A3	2.07	2.60	220	88.8
A4	1.48	2.35	215	94.6
Begin	5.10	10.04	209	
B1	3.76	7.76	210	89.7
B2	2.40	6.10	208	90.6
B3	1.55	4.28	207	89.2
B4	1.10	3.40	207	89.7
B5	0.68	2.97	204	87.5
B6	0.50	2.16	202	88.0
B7	0.38	1.93	200	89.6
B8	0.28	1.57	200	89.0

case is 5.9×10^{12}. While several parameters of the aforementioned scheme such as the rf gradient, window thickness, focusing field still need to be evaluated for practicality and cost the aforementioned facts suggest that the rectilinear channel has the potential to be a promising solution.

In Fig. 10 we plot the transverse and longitudinal emittances as a function of distance along the channel for the section after the bunch recombination. The solid lines depict the estimated emittances from ICOOL while the black squares depict the theoretical results from Eq. (9).

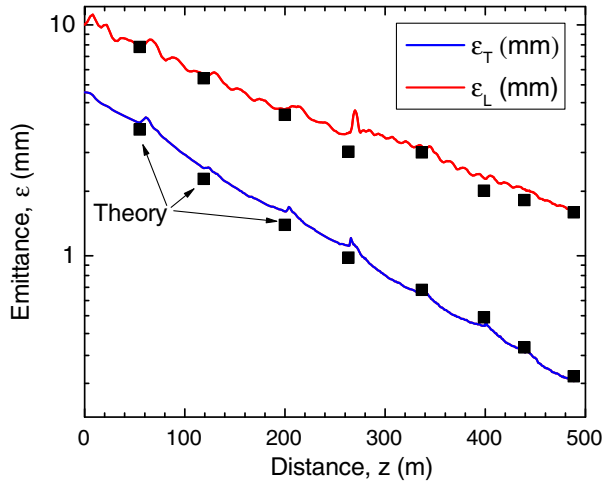

FIG. 10. Simulation results and theoretical predictions of the performance of a rectilinear 6D cooling channel for a muon collider. The plot shows the evolution of the normalized rms emittances as a function of distance along the channel after recombination. At $z = 488$ m the transmission is 40% with muon decays, while the final simulated emittances are $\varepsilon_T^{\mathrm{sim}} = 0.28$ mm and $\varepsilon_L^{\mathrm{sim}} = 1.57$ mm. The squares are theoretical calculations from Eq. (9). The agreement between theory and simulation is within 18%.

TABLE III. Performance of a 6D rectilinear channel after bunch recombination based on theory. Emittances are calculated from Eq. (9) while the cooling lengths s^{calc} are calculated from Eqs. (10) and (11). The error between theory and simulation (from Table II) is less than 18%. The theoretical numbers are based on using the initial values in each stage that were obtained from the simulation of the previous stage.

Stage	s_T^{calc} [m]	s_L^{calc} [m]	$\varepsilon_T^{\mathrm{calc}}$ [mm]	$\varepsilon_L^{\mathrm{calc}}$ [mm]
B1	67.9	200.4	3.52	8.06
B2	53.6	168.1	2.16	5.87
B3	49.7	137.8	1.35	4.07
B4	45.3	99.3	0.98	2.89
B5	28.5	164.4	0.71	2.80
B6	26.2	78.6	0.53	1.91
B7	30.5	84.2	0.40	1.74
B8	32.1	86.6	0.30	1.55

The theoretical values of the emittances at the exit of each stage are also shown in Table III. A comparison between theory and simulation is a key step since a well-designed channel must accurately follow the predictions. Deviations are usually associated with poor dynamic acceptance, chromatic effects, or poor matching into the channel [35]. A glance at Fig. 10 indicates that the linear theory presented in Sec. IV predicts relatively well the cooling performance of our rectilinear channel. Quantitatively, the error between the theoretical values and numerical results is less than 18%. The most likely source of discrepancy at 263.5 m is mismatch caused by the rf frequency shift from 325 MHz to 650 MHz at that point.

VI. SUMMARY

For a muon collider, the six-dimensional phase space volume of the initial muon beam must be reduced by several orders of magnitude in order to be able to further accelerate it. Ionization cooling is the only feasible option for cooling within the short muon lifetime ($\tau_0 = 2.2$ μs). In this study, we have described a novel rectilinear lattice that in view of its simple geometry may offer several technological advantages for beam cooling over previously considered schemes [13]. Unlike previous studies where an *a priori* assumption of the initial beam distribution was made [27] and/or a modest cooling was achieved, in this paper we have presented a detailed end-to-end simulation by using the actual post-phase-rotation beam and showed that our channel has the potential to cool towards micron-scale transverse emittances as desired for a muon collider. We showed that relatively modest magnetic fields ($B \leq 13.6$ T, peak on axis) and a small number of different frequencies, namely 325 and 650 MHz, are enough to achieve a notable reduction of the 6D emittance by more than 5 orders of magnitude. Finally, we have reviewed the key theoretical framework to evaluate the performance of ionization cooling channels and discussed its application to our present rectilinear scheme. Key theoretical findings,

such as the cooled transverse and longitudinal emittances, were found to agree closely with the results from numerical simulations. We conclude that while several parameters of the aforementioned scheme such as the rf gradient, absorber type, window thickness and focusing field still need to be evaluated for practicality and cost the present study indicates that a Balbekov-based rectilinear scheme [20] is a promising 6D cooling solution for a muon collider.

ACKNOWLEDGMENTS

The authors are grateful to Y. Bao, J. S. Berg, F. Borgnolutti, D. Bowring, X. Ding, D. Grote, S. Khan, T. Luo, H. K. Sayed, K. Yonehara, C. Yoshikawa, and H. Witte for many useful discussions. This work is supported by the U.S. Department of Energy, Contract No. DE-AC02-98CH10886.

[1] M. Tigner, AIP Conf. Proc. **279**, 1 (1992).
[2] J. D. Jackson, *Classical Electrodynamics*, 3rd ed. (Wiley, New York, 1999).
[3] G. I. Budker, in *Proceedings of the 7th International Conference on High-Energy Accelerators, Yerevan, 1969* (Academy of Sciences of Armenia, Yerevan, 1970), p. 33.
[4] A. N. Skrinsky and V. V. Parkhomchuk, *Sov. J. Part. Nucl.* ***12****, 223 (1981).*
[5] C. M. Ankenbrandt *et al.*, Phys. Rev. ST Accel. Beams **2**, 081001 (1999).
[6] R. B. Palmer *et al.*, in *Proceedings of the 22nd Particle Accelerator Conference, PAC-2007, Albuquerque, NM* (IEEE, New York, 2007), p. 3193.
[7] Yu M. Ado and V. I. Balbekov, Atomic Energy **31**, 731 (1971).
[8] D. Neuffer, *Part. Accel.* ***14****, 75 (1983).*
[9] D. Neuffer, Nucl. Instrum. Methods Phys. Res., Sect. A **532**, 26 (2004).
[10] V. I. Balbekov and A. Van Ginneken, *AIP Conf. Proc.* 441, 310 (1998).
[11] Y. Alexahin, AIP Conf. Proc. **1222**, 313 (2010).
[12] Y. Derbenev and R. P. Johnson, Phys. Rev. ST Accel. Beams **8**, 041002 (2005).
[13] P. Snopok, G. Hanson, and A. Klier, Int. J. Mod. Phys. A **24**, 987 (2009).
[14] J. Pasternak, Nucl. Phys. B, Proc. Suppl. **149**, 271 (2005).
[15] R. C. Fernow, in *Proceedings of the 21st Particle Accelerator Conference, Knoxville, TN, 2005* (IEEE, Piscataway, NJ, 2005), p. 2651.
[16] C. T. Rogers, D. Stratakis, G. Prior, S. Gilardoni, D. Neuffer, P. Snopok, A. Alekou, and J. Pasternak, Phys. Rev. ST Accel. Beams **16**, 040104 (2013).
[17] R. Palmer, V. Balbekov, J. S. Berg *et al.*, Phys. Rev. ST Accel. Beams **8**, 061003 (2005).
[18] A. Klier and G. G. Hanson, Neutrino factory/Muon Collider Document No. 298 (2004).
[19] P. Snopok and G. Hanson, in *Proceedings of the 23rd Particle Accelerator Conference, Vancouver, Canada, 2009* (IEEE, Piscataway, NJ, 2009), p. 4381.
[20] V. Balbekov, Muon Accelerator Program Document No. 4365 (2013), http://map-docdb.fnal.gov.
[21] D. Stratakis *et al.*, in *Proceedings of the 2014 IPAC, Dresden, Germany* (International Particle Accelerator Conference (IPAC), Dresden, Germany, 2014), p. 1389.
[22] C. Yoshikawa *et al.*, in *Proceedings of the 25th Particle Accelerator Conference, PAC-2013, Pasadena, CA, 2013* (IEEE, New York, 2013), p. 1343.
[23] R. B. Palmer and R. C. Fernow, in *Proceedings of the 24th Particle Accelerator Conference, PAC-2011, New York, 2011* (IEEE, New York, 2011), p. 103.
[24] R. B. Palmer and R. C. Fernow, in *Proceedings of the 3rd International Particle Accelerator Conference, New Orleans, LA, 2012* (IEEE, Piscataway, NJ, 2012), p. 1831.
[25] R. B. Palmer and R. C. Fernow, in *Proceedings of the 24th Particle Accelerator Conference, PAC-2011, New York, 2011* (Ref. [23]), p. 109.
[26] Y. Bao and R. B. Palmer, Bunch-Merge Status, *Vacuum Cooling Channel Workshop II (Batavia, IL, 2013), https://indico.fnal.gov/conferenceDisplay.py?confId=7586.*
[27] R. B. Palmer and R. C. Fernow, in *Proceedings of the 24th Particle Accelerator Conference, PAC-2011, New York, 2011* (Ref. [23]), p. 106.
[28] V. I. Balbekov, in *Proceedings of the 18th Particle Accelerator Conference, New York, 1999* (IEEE, New York, 1999), p. 315.
[29] D. Stratakis, R. C. Fernow, J. S. Berg, and R. B. Palmer, Phys. Rev. ST Accel. Beams **16**, 091001 (2013).
[30] D. Neuffer, Muon Accelerator Program Document No. 4371 (2013), http://map-docdb.fnal.gov.
[31] http://fs.magnet.fsu.edu/~lee/plot/plot.htm.
[32] H. Witte, D. Stratakis, J. S. Berg, and F. Borgnolutti, in *Proceedings of the 2014 IPAC, Dresden, Germany* (2014), p. 2740, http://accelconf.web.cern.ch/AccelConf/IPAC2014/html/author.htm.
[33] S. Prestemon, Magnet Requirements and Limitations, *Muon Accelerator Program Spring Meeting* (Batavia, IL, 2014), https://indico.fnal.gov/conferenceOtherViews.py?view=standard&confId=8326.
[34] E. Keil, Muon cooling channels, Report No. FERMILAB-TM-2196, 2003.
[35] D. Neuffer, Neutrino factory/Muon Collider Document No. 227 (2001), http://nfmcc-docdb.fnal.gov/cgi-bin/DocumentDatabase/.
[36] C. Caso *et al.*, *Eur. Phys. J. C* ***3****, 1 (1998).*
[37] U. Fano, Annu. Rev. Nucl. Sci. **13**, 1 (1963).
[38] See Eqs. (11), and (16) in R. C. Fernow, Neutrino Factory/Muon Collider Document No. 280 (2003), http://nfmcc-docdb.fnal.gov/cgi-bin/DocumentDatabase/.
[39] D. Stratakis *et al.*, in *Proceedings of the 4th International Particle Accelerator Conference, IPAC-2013, Shanghai, China, 2013* (JACoW, Shanghai, China, 2013), p. 1553.
[40] J.-P. Delahaye, R. B. Palmer, T. J. Roberts, R. Ryne, M. J. Syphers, and K. Yonehara, Criteria for comparing, and assessing 6-D cooling channels, Muon Accelerator Program internal document, version dated February 10, 2014.
[41] R. B. Palmer, Draft muon collider parameters, Muon Accelerator Program Document No. 4318 (2011), http://map-docdb.fnal.gov.